



Full paper/Mémoire  
Epoxy-functionalized large-pore SBA-15 and KIT-6  
as affinity chromatography supports

Nathalie Calin<sup>a</sup>, Anne Galarneau<sup>a,\*</sup>, Thomas Cacciaguerra<sup>a</sup>,  
Renaud Denoyel<sup>b</sup>, François Fajula<sup>a</sup>

<sup>a</sup> CNRS/UM2/ENSCM/UM1 UMR 5253 « Matériaux avancés pour la catalyse et la santé », institut Charles-Gerhardt,  
8, rue de l'École-Normale, 34296 Montpellier cedex 5, France

<sup>b</sup> CNRS UMR 6121 Madirel, centre Saint-Jérôme, université de Provence, avenue Escadrille-Normandie-Niemen,  
13397 Marseille cedex 20, France

Received 26 January 2009; accepted after revision 15 April 2009

Available online 12 June 2009

## Abstract

Mesoporous silica supports are proposed as an alternative to polymeric stationary phases for fast affinity chromatography due to their better mechanical strength compared to polymers. Ideal supports should combine high surface area and large pore size to allow a high loading capacity of large molecules, such as proteins, and favor their accessibility. Increasing the pore size of large-surface area micelle-templated silicas (SBA-15, KIT-6) has been achieved by swelling the micelles by the addition of organic molecules and increasing synthesis time and temperature. The pore size of hexagonal silica mesostructured SBA-15 has been increased up to 35 nm. These materials could find therefore application as affinity chromatography for immunoextraction. **To cite this article:** *N. Calin et al., C. R. Chimie 13 (2010).*

© 2009 Published by Elsevier Masson SAS on behalf of Académie des sciences.

## Résumé

Des silices mésoporeuses sont proposées comme supports pour la chromatographie d'affinité en remplacement des matrices polymériques en raison de leur meilleure stabilité mécanique. Les supports idéaux se caractérisent par une surface spécifique et des diamètres de pores élevés pour permettre une grande capacité d'immobilisation de larges molécules, telles les protéines, et une bonne accessibilité à celles-ci. La préparation de silices mésoporeuses structurées de type SBA-15 et KIT-6 possédant de grandes surfaces spécifiques et des diamètres de pores élevés a été réalisée par l'addition d'auxiliaires organiques aux micelles de structuration. La taille des pores de silices mésostructurées de symétrie hexagonale de la famille des SBA-15 a ainsi été augmentée jusqu'à 35 nm. Ces matériaux pourraient constituer des candidats potentiels pour les procédés d'immunoextraction. **Pour citer cet article :** *N. Calin et al., C. R. Chimie 13 (2010).*

© 2009 Publié par Elsevier Masson SAS pour l'Académie des sciences.

**Keywords:** SBA-15; KIT-6; Affinity chromatography support; Mesoporous silica

**Mots clés :** SBA-15 ; KIT-6 ; Supports pour la chromatographie d'affinité ; Silices mésoporeuses

## 1. Introduction

High-performance affinity chromatography (HPAC) is gaining more and more interest for the separation and

\* Corresponding author.

E-mail address: [anne.galarneau@enscm.fr](mailto:anne.galarneau@enscm.fr) (A. Galarneau).

analysis of biological compounds with industrial or environmental interest. HPAC is derived from the high-performance liquid chromatographic (HPLC) technique and involves supports modified by specific binding agents (IgG antibodies, protein A or other biometric ligands) [1]. Examples of HPAC applications include chromatographic-based immunoassays, on-line immunoextraction and multidimensional schemes in which antibody affinity columns are coupled with reversed-phase liquid chromatography, gas chromatography or capillary electrophoresis [2–6]. There are several ways that antibodies and other proteins can be attached to HPLC supports for use in affinity columns [2,3,5–9]. High-density of antibodies or proteins grafted affinity supports are needed to develop small columns or to promote fast, quantitative binding of analytes. Such evolution should become particularly important as current trends continue in micromachining and in the development of miniaturized separation systems. The interactions that occur in affinity chromatography are identical to those occurring in many biological systems, such as the binding of an enzyme with a substrate or of an antigen with an antibody. The specific nature of these interactions gives affinity chromatography a high degree of selectivity.

Among the factors that affect the performance in HPAC, the surface area of the supports and the size of the pores within the support play a dominant role in determining the amount of immobilized antibodies or proteins that are accessible for the binding of the analytes. Cross-linked polysaccharides, agarose, sepharose, cellulose or other synthetic polymers (polystyrene vinyl benzene) are widely used as support matrices. Silica matrices can be alternatives for high-throughput in HPAC as they develop better mechanical strength and can therefore stand higher pressure for fast separation processes. The main challenge in using silica supports in HPAC is, however, the necessity to combine a large pore with a high surface area.

In the case of immunoglobulin (IgG) immobilization, as an IgG molecule has an average diameter of 8–10 nm, supports should develop a pore size larger than 10 nm. A comparison of a series of HPLC-grade silica supports led to the conclusion that maximum performance corresponded to materials featuring a pore size of 30 nm and a surface area of 100 m<sup>2</sup>/g. The benefit of increasing pore size was lost by the concurrent decrease of surface area [10]. As an example, in the case of 30 nm pore-sized silica, 1.7 μmol IgG/g silica were grafted, and the use of silica support with pore size of 50 nm ( $S = 35 \text{ m}^2/\text{g}$ ) led to a density of 0.9 μmol IgG/g silica. For smaller proteins ( $\approx 4\text{--}5 \text{ nm}$ ), it was demonstrated

that a maximum grafting is obtained for a support with pore sizes two or three times the diameter of the proteins [10]. Therefore, there is a need for supports with pore sizes between 10 and 30 nm featuring high surface area.

Micelle-templated silica materials (MTS) are known to develop very high surface area up to 900–1000 m<sup>2</sup>/g [11]. To be used as HPLC supports a morphological control should be added to the classical synthesis to reach homogeneous particle-size distribution. We have shown recently that these ordered mesoporous silicas with hexagonal or cubic symmetry, such as MCM-41 or MCM-48, produced by a pseudomorphic transformation [12–17] of commercial chromatography supports led to significant performance improvements in HPLC [18]. The pore sizes of the MTS materials investigated stand however in the range 4–7 nm, which is indeed not appropriate for HPAC application. These MTS synthesis were using cetyltrimethylammonium (CTMA) as surfactant and trimethylbenzene (TMB) as swelling agent in alkaline media. The use of another kind of surfactant such as triblock copolymer EO<sub>20</sub>EO<sub>70</sub>EO<sub>20</sub> in acidic media led to other MTS types, namely SBA-15 [19–23] and KIT-6 [24,25], with 8–9 nm pore size. Some attempts have been made to make spherical particles of SBA-15, but aggregation of particles could not be avoided [26]. The use of TMB as swelling agent combined with EO<sub>20</sub>EO<sub>70</sub>EO<sub>20</sub> led to the formation of a silica material, named mesocellular foam (MCF), featuring a three-dimensional pore structure with large cavities (20–50 nm) interconnected by windows (9–26 nm) [27–29]. For HPLC support materials, we have previously shown that support with cavities should be avoided, and that the best supports should present uniform pore sizes [12].

The main objective of this work was therefore to examine the possibility to produce MTS with uniform pore distributions, with pore sizes in the range: 15–30 nm and surface areas larger than those achievable with traditional HPLC supports. Moreover, we have previously shown that the more efficient activated groups to bind proteins on silica, and more precisely on MTS materials, were glycidoxy groups [30]. We report here our results on the synthesis, the characterization and the epoxy-functionalization of large-pore mesostructured silicas from the families of SBA-15 [19–23] and KIT-6 [24,25].

## 2. Experimental section

### 2.1. SBA-15 and SBA-15/TMB

The synthesis procedure of large-pore silicas with hexagonal symmetry ( $P_{6mm}$ ), named SBA-15, uses

triblock-copolymer pluronic P123 ( $\text{EO}_{20}\text{PO}_{70}\text{EO}_{20}$ , Aldrich) as surfactant in the presence of TMB. The synthesis protocols were adapted from reference [23]. The synthesis procedure is the following: 2 g of pluronic P123, 52 g  $\text{H}_2\text{O}$  and 10 mL HCl 35% are stirred for 30 min. Subsequently, 4.3 g of TEOS (equivalent to 1.24 g of silica) and 0 or 2 g of TMB are then added. The mixture is stirred at 35 °C for 24 h and left in static at different temperatures (100 to 130 °C) for different times (1 to 3 days) in closed PFA bottles. The synthesis mixture corresponds to the molar ratio of: 1  $\text{SiO}_2$ /0.017 P123/5.6 HCl/0 or 0.81 TMB/140  $\text{H}_2\text{O}$ . The slurry is then filtered, washed rapidly with water and dried under vacuum at room temperature. The materials are then calcined at 550 °C for 8 h. After calcination 1.2 g of large-pore SBA-15 are obtained corresponding to a silica yield close to 90%.

## 2.2. KIT-6 and KIT-6/TMB

The synthesis procedure of large-pore silica materials with cubic  $I_{a3d}$  symmetry, named KIT-6, used a mixture of tribloc-copolymer pluronic P123 and butanol as structuring agents. The synthesis protocol was adapted from references [24] and [25]. The synthesis procedure is the following: 2 g of pluronic P123 (Aldrich), 72 g  $\text{H}_2\text{O}$  and 3.4 mL HCl 35% are stirred at 35 °C for 30 min to obtain a clear solution. Subsequently, 2 g butanol are added and the mixture is stirred for 1 h. Then 4.3 g of TEOS (equivalent to 1.24 g of silica) are added, and the mixture is stirred at 35 °C for 24 h and left in static at different temperatures (100 to 130 °C) for different times (1 to 3 days) in Teflon or PFA bottles. The synthesis mixture corresponds to the molar ratio of: 1  $\text{SiO}_2$ /0.017 P123/1.9 HCl/1.3 butanol/194  $\text{H}_2\text{O}$ . The slurry is then filtered, dried at 100 °C for 24 h. A rapid washing is done with a HCl/EtOH solution before calcination. The materials are then calcined at 550 °C for 8 h. After calcination, 1 g of large-pore KIT-6 silicas is obtained corresponding to a silica yield close to 80%. KIT-6/TMB materials were obtained by adding TMB to the above reaction mixture using a molar ratio TMB/Si of 0.8.

## 2.3. Epoxy-activated silica

In a flask of 250 mL, 3 g of silica are left for 60 min at room temperature under argon flow to remove a part of the adsorbed water molecules. Then 30 mL of anhydrous toluene are added together with amounts of glycidoxy propyltrimethoxysilane corresponding to 1.5 epoxy groups/ $\text{nm}^2$  of dried silica. The mixture is heated under reflux at 120 °C under magnetic stirring

and under argon flow for 1 h 30 min. The hydrolysis of the methoxy silane leads to the formation of methanol, which is continuously distilled with a Dean Stark. The reaction mixture is stirred for another 1 h 30 min at 120 °C under argon. The resulting solid is then filtered and washed with anhydrous toluene, and then in a Soxhlet with a ether/dichloromethane mixture (1/1 in volume) at 60 °C overnight. The epoxy-activated silica is then dried in the oven at 60 °C for 1 day.

## 2.4. Characterizations

Powder X-ray diffraction patterns were collected on a CGR Thêta-60 diffractometer with Inel drive, using monochromatic Cu  $K\alpha$  radiation and four 0.25 mm slits. The particle morphology was observed using a Hitachi S-4500 I scanning electron microscope (SEM). The particle size distribution was determined by laser diffraction (Mastersizer 2000 from Malvern Instruments): 200 mg of sample was added to 10 mL of acetone, ultrasonicated for 30 min, dried, and dispersed into 700 mL of water for analysis. The ordering of silica network was examined by transmission electron microscopy (TEM) images obtained using a Philips CM 20 apparatus operating at 100 keV. Nitrogen sorption isotherms at 77 K were determined with an ASAP2010 apparatus from Micromeritics. Before measurement, the samples were outgassed under vacuum at 250 °C for silicas. The BET equation was applied to determine the surface area. Average pore diameters have been evaluated from the nitrogen desorption branch according to the Broekhoff and De Boer (BdB) method [31], as this method has been demonstrated to be one of the more accurate method to evaluate pore size [32]. High-resolution thermogravimetry under nitrogen gas flow was used in order to calculate the density of hydroxyl groups existing on the surface of the calcined samples (pure silica). Assuming that, after outgassing at 150 °C, most OH groups are still on the surface, it is possible to derive their amount from the mass loss between 150 and 850 °C. The TG analyses were achieved by a TGA Q500 apparatus from TA Instruments. The high-resolution program was followed from 30 to 850 °C. In order to determine the epoxy density on the silicas, thermogravimetric analysis (TGA) was recorded also under an oxygen flux on a TG 209C analyser (Netzsch Proteus). Adsorption isotherms of water vapour at 25 °C were determined with a home-made apparatus based on a symmetrical commercial vacuum microbalance from Setaram [33]. The samples were preliminary evacuated under vacuum at 120 °C for 12 h.

### 3. Results and discussion

#### 3.1. Large-pore SBA-15 and KIT-6

The synthesis of SBA-15 in the absence of TMB at 130 °C for 1 day produced a material with 8 nm pore diameter and a surface area of 550 m<sup>2</sup>/g (Table 1, sample 1). The synthesis conditions have been chosen to avoid the presence of microporosity [21,22]. This explains why the surface area stands around 500 m<sup>2</sup>/g, a value significantly lower than that reported (900 m<sup>2</sup>/g and above) in most of the cases for SBA-15-type materials (synthesized at lower temperature).

The addition of TMB to the reaction mixture and the use of different temperatures and times of reaction resulted in the series of materials presented in Table 1, featuring pore sizes in the range 8 to 35 nm. The nitrogen adsorption/desorption isotherms reveal an

increase in pore volume and a decrease in surface area from 500 to 300 m<sup>2</sup>/g upon increasing the pore size. The obtained surface areas for these materials are two to three times higher than those of traditional silicas with similar pore size, which means that their loading capacity should also be increased by the same factor. It is interesting to note that in our synthesis using TMB as swelling agent, the uniformity of the pores and their cylindrical shape is maintained, as characterized by the steep step in the adsorption and desorption branches of nitrogen isotherms and the narrow hysteresis loop with parallel adsorption and desorption branches as shown on Fig. 1. The hexagonal symmetry is preserved for the whole series of materials, as exemplified by the XRD pattern at low angle of sample 5 (Fig. 2), except for sample 7 with a pore diameter of 35 nm, which shows a lower degree of ordering. These materials differ therefore from the MCF reported by Stucky et al.

Table 1

Features of calcined large-pore silicas with hexagonal symmetry SBA-15 and SBA-15/TMB: surface area, pore volume and pore diameter determined by nitrogen adsorption/desorption volumetry, d-spacing determined by XRD.

Sample no.	Type	T (°C)	Time (days)	S (m <sup>2</sup> /g)	V (mL/g)	D (nm)	d <sub>XRD</sub> (nm)
1	SBA-15	130	1	550	0.97	8	9.3
2	SBA/TMB	100	1	620	1.80	11	18
3	SBA/TMB	100	3	459	1.78	14	26
4	SBA/TMB	120	3	461	1.58	14	23
5	SBA/TMB	130	3	417	2.03	19	24
6	SBA/TMB	130	5	299	2.25	25	24
7	SBA/TMB	130	6	302	2.46	35	> 29

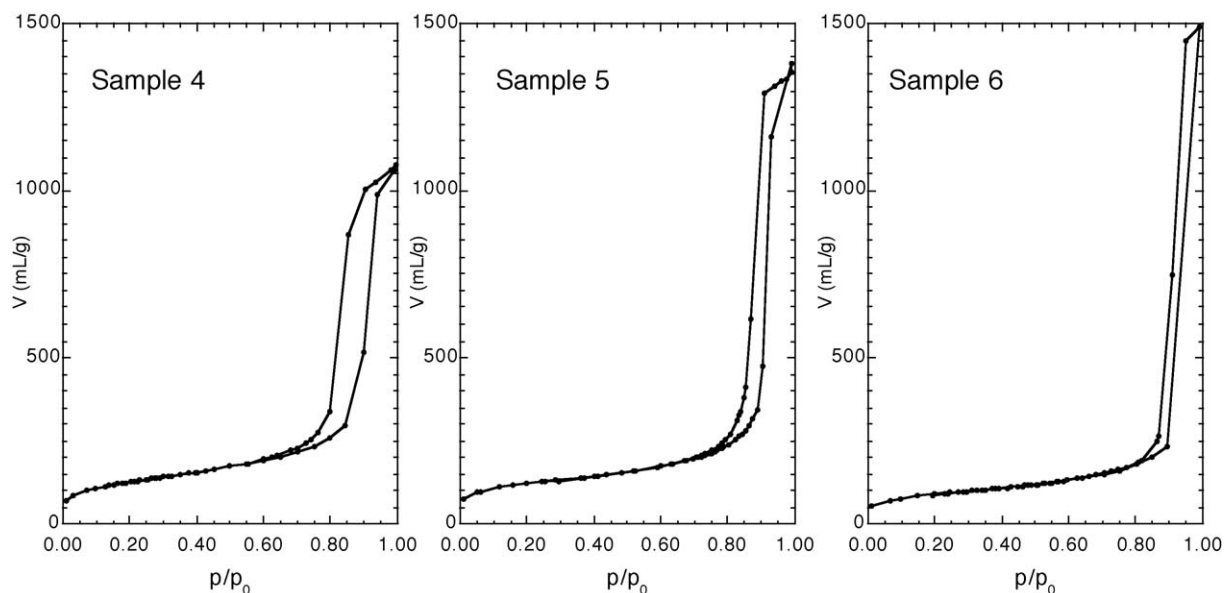


Fig. 1. Nitrogen adsorption/desorption isotherms at 77 K of large-pore SBA-15/TMB materials synthesized at 120 °C for 3 days (sample 4), at 130 °C for 3 days (sample 5) and at 130 °C for 5 days (sample 6).

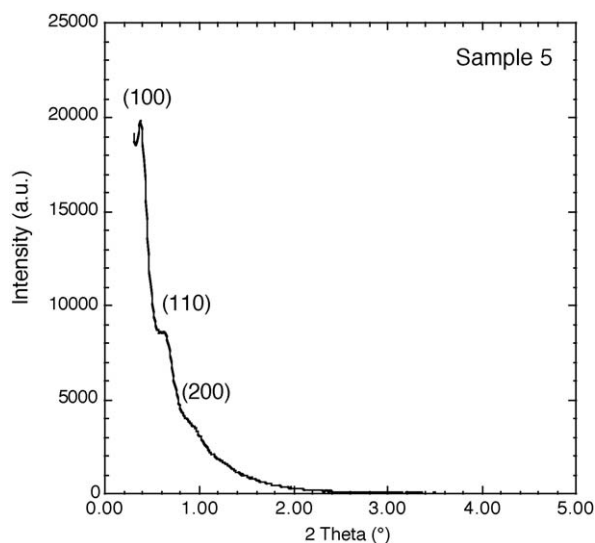


Fig. 2. X-ray diffraction pattern of calcined large-pore SBA-15/TMB materials synthesized at 130 °C for 3 days (sample 5).

[27,28] which feature large hysteresis loops due to the presence of cavities and windows. TEM images (Fig. 3a) confirm the well ordered hexagonal arrangement of the pores and their uniformity throughout the grains. The large-pore SBA-15 particles exhibit a raspberry shape (Fig. 3b) with a narrow distribution of sizes, as determined by PSD measurements (Fig. 3c). Among the materials produced, sample 6 obtained at

130 °C after 5 days of reaction shows most interesting features in view of its potential application in HPAC: a pore diameter of 25 nm, a surface area of 300 m<sup>2</sup>/g and a narrow particle size distribution of  $11 \pm 5 \mu\text{m}$ . Besides the textural properties, particle size is also an important characteristic for chromatography applications to induce a good column packing and optimize mass transfer.

The synthesis of KIT-6 materials in the absence of TMB as swelling agent at 100–130 °C and 1 to 6 days of reaction produces materials with pore sizes in the range: 8–11 nm and surface areas of 500–600 m<sup>2</sup>/g (Table 2, samples 8–12). Nitrogen adsorption/desorption isotherms show the uniformity of the pores, characterized by a steep step in the isotherm and a narrow hysteresis loop (Fig. 4a). The XRD patterns (Fig. 5) as well as the TEM pictures (Fig. 6a) confirm the conservation of the cubic symmetry. SEM pictures (not shown) reveal that the materials are formed of grains with irregular shape leading to a nonuniform broad distribution of particle sizes around  $17 \pm 11 \mu\text{m}$ . The addition of TMB to the KIT-6 synthesis mixture results in a loss of the cubic symmetry and does not allow a significant increase of the pore size (samples 13–17, Table 2). XRD patterns do not show any long-range ordering and the nitrogen adsorption isotherm shows a less steep adsorption step, indicating a broader pore size distribution (Fig. 4b). TEM pictures show that the structural and textural characteristics of the material have completely changed.

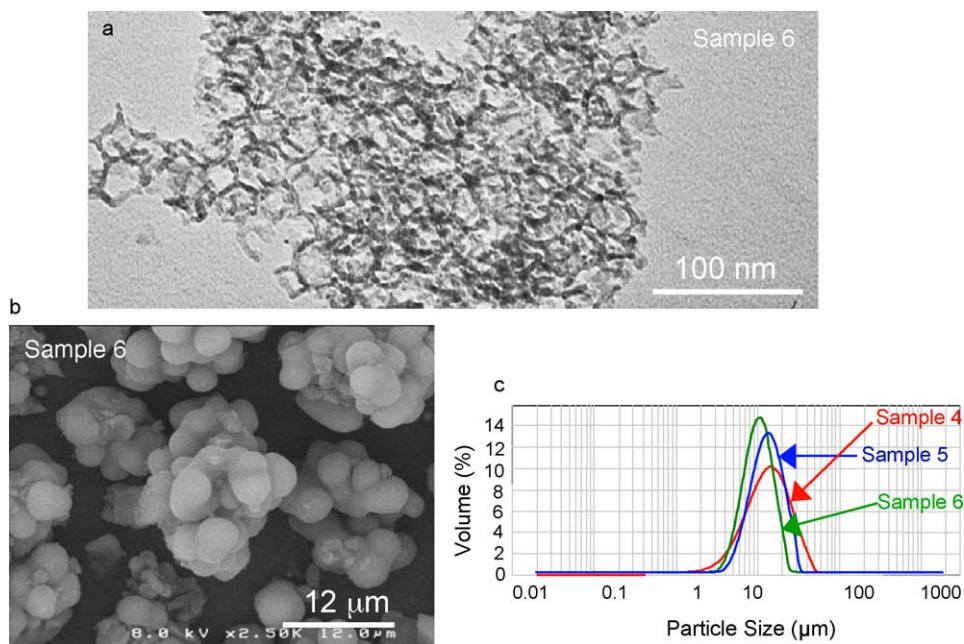


Fig. 3. a: TEM picture; b: SEM picture and c: particle size distributions of calcined large-pore SBA-15/TMB materials.

Table 2

Features of calcined large-pore silicas with cubic symmetry KIT-6 and KIT-6/TMB: surface area, pore volume and pore diameter determined by nitrogen adsorption/desorption volumetry, d-spacing determined by XRD.

Samples no.	Type	T (°C)	Time (days)	S (m <sup>2</sup> /g)	V (mL/g)	D (nm)	d <sub>XRD</sub> (nm)
8*	KIT-6	100 (PFA)	1	622	0.91	8	9.2
9	KIT-6	100 (Teflon)	1	542	1.30	10	9.2
10	KIT-6	115	6	609	1.28	10	8.6
11	KIT-6	130 (Teflon)	3	488	1.32	11	9.2
12	KIT-6	130	4	535	1.30	10	9.5
13	KIT/TMB	100	1	716	0.98	12	Amorphous
14	KIT/TMB	115	6	530	1.57	16	Amorphous
15	KIT/TMB	120	1	585	1.40	10	Amorphous
16	KIT/TMB	120	3	456	1.26	12	Amorphous
17	KIT/TMB	130 (PFA)	4	353	1.20	14	Amorphous

\*without intermediate washing by a HCl–EtOH mixture.

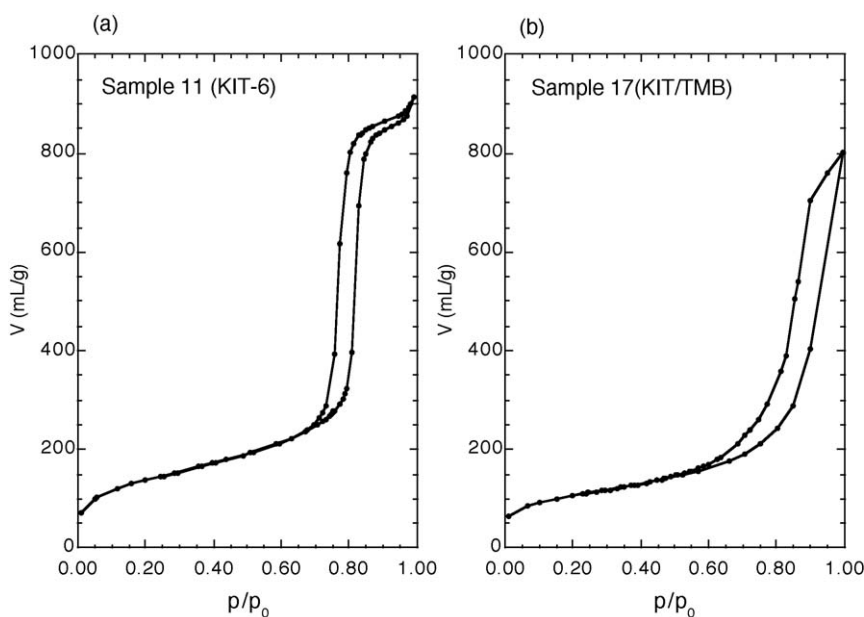


Fig. 4. Nitrogen adsorption/desorption isotherms at 77 K of large-pore KIT-6 and KIT-6/TMB materials.

All KIT-6 samples prepared with TMB form as vesicles, probably built of ribbons of silicate layers (Fig. 6b). Moreover, particle size distributions become broader, around  $17\text{--}25 \pm 17 \mu\text{m}$ .

### 3.2. Surface properties

TGA measurements performed on calcined materials reveal that all the large-pore silicas prepared in this study feature a low-density of silanol groups, especially in the case of the cubic structures of KIT-6 type (Table 3). For SBA-15 and SBA-15/TMB, the density of silanol groups stands between 2 and  $2.6 \text{ SiOH/nm}^2$ , while for KIT-6 and KIT-6/TMB a value around  $1.2\text{--}1.5 \text{ SiOH/nm}^2$  is obtained. Water adsorption isotherms confirm the low

polarity of the surfaces. The shapes of the isotherms are more of the type III of the Brunauer isotherms classification [34], indicating a very low affinity of the surface for water molecules, rather than of type I as generally observed for hydroxylated silicas. It is therefore not fully appropriate to use the BET transformation [34] to evaluate a monolayer water coverage because the BET transformation curves show very low or no linearity in the range:  $0.05 < p/p_0 < 0.2$ . Nevertheless, some calculations have been conducted to evaluate a monolayer coverage from the linear parts of the BET transformations between  $0.1 < p/p_0 < 0.4$  for SBA materials and between  $0.2 < p/p_0 < 0.4$  for KIT-6, where a sufficient amount of water could cover the surface. Around  $3\text{--}4 \text{ H}_2\text{O/nm}^2$  have been approximated for

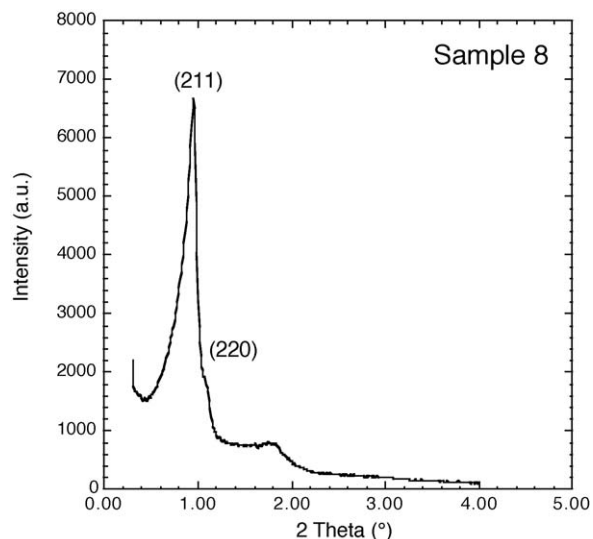


Fig. 5. X-ray diffraction pattern of calcined large-pore KIT-6 materials.

SBA-type materials and around 2–3  $\text{H}_2\text{O}/\text{nm}^2$  for KIT-type materials. The correlation with silanol density seems therefore to be of two water molecules per silanol group. In SBA-type materials, and more particularly in KIT-type materials, the silanol groups should be located far apart from each other leading to isolated hydrophobic silanol groups.

In spite of the difference in density of surface silanol groups found on the two series of materials, a similar level of grafting of glycidoxypropylsilane, corresponding to a density of  $0.56 \pm 0.10$  epoxy/ $\text{nm}^2$ , was achieved for all samples, as shown in Table 4. Taking into account the surface areas developed or the density of the samples, these materials feature immobilized epoxy amounts suitable to graft bulky molecules such as antibodies adjustable between 300 and 550  $\mu\text{mol}/\text{g}$  of silica or between 80 and 170  $\mu\text{mol}/\text{mL}$  of column. These values are close to those of the commercial polymeric stationary phases used in affinity chromatography. Large-pore

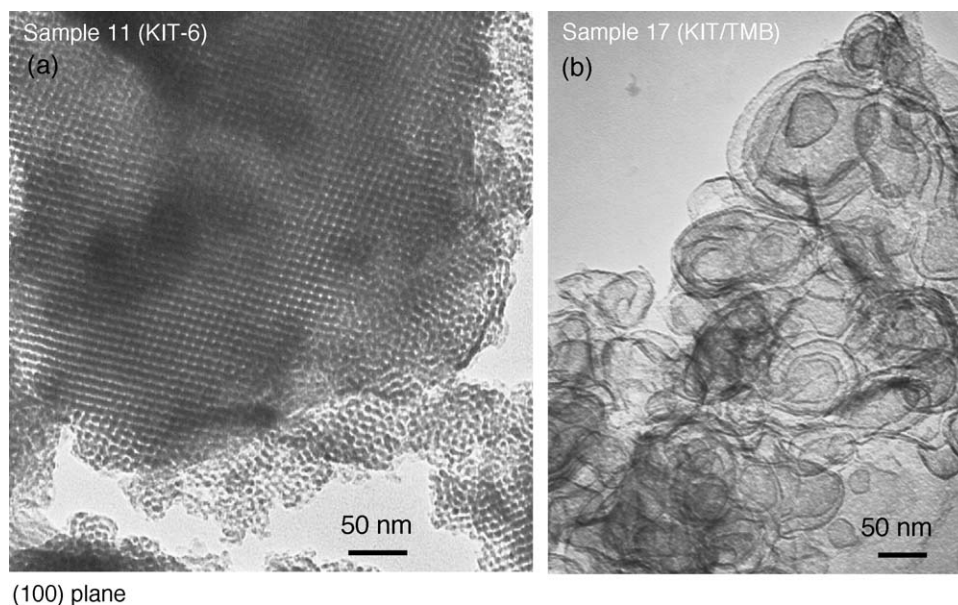


Fig. 6. TEM pictures of large-pore (a) KIT-6 and (b) KIT-6/TMB materials.

Table 3  
Bulk and surface characterization of SBA-15, SBA/TMB, KIT-6, KIT/TMB.

Samples no.	Type	S ( $\text{m}^2/\text{g}$ )	Water weight loss 200–800 °C mg/g silica	SiOH (TGA) mmol/g	SiOH/ $\text{nm}^2$ (TGA)	Water ads at $p/p_0 = 0.4$ $\text{H}_2\text{O}/\text{nm}^2$	Water ads at monolayer coverage $\text{H}_2\text{O}/\text{nm}^2$
1	SBA-15	550	16.2	1.80	1.96	3.3	2.9
18	SBA/TMB	259	10.3	1.14	2.64	3.9	4.9
10	KIT-6	609	10.6	1.18	1.16	2.0	2.5
12	KIT-6	535	12.2	1.34	1.52	2.3	2.1
14	KIT/TMB	530	11	1.22	1.38	2.6	2.8

Sample 18: 115 °C/6 days, scale-up synthesis ( $\times 4$ ).

Table 4

Density of the samples and amount of epoxy grafted on SBA-15, SBA/TMB, KIT-6, KIT/TMB samples.

Samples no.	Type	Density (g/cm <sup>3</sup> )	Surface area (m <sup>2</sup> /g)	3-glycidoxy propylsilane (μmol/g)	molecule/nm <sup>2</sup>
1	SBA-15	0.26	550	543	0.59
5	SBA/TMB	0.22	417	306	0.44
18	SBA/TMB		259	294	0.69
19	SBA/TMB	0.21	345	375	0.66
12	KIT-6	0.33	535	451	0.51
11	KIT-6	0.24	488	433	0.53
14	KIT/TMB	0.35	530	483	0.55

Sample 19: scale-up synthesis (× 4) of sample 5.

SBA-15 type materials could therefore compete with traditional chromatographic support phases.

#### 4. Conclusion

Large-pore high surface area silica materials have been prepared by adapting the synthesis conditions of MTS of the SBA-15 and KIT-6 families. The most relevant results in terms of possible application in the field of HPAC have been obtained with the SBA-15 series. Pore sizes have been increased from 8 to 25 nm while maintaining a surface area of 300 m<sup>2</sup>/g or above and a very narrow distribution of pore and particle sizes. Surface functionalization with glycidoxypropylsilane allowed to produce supports with a high density of epoxy groups prone to immobilize bulky biological ligands such as antibodies or proteins.

#### Acknowledgements

Authors thank the European council for financial support through European Integrative Project of FP6 named “Advanced interactive materials by design” (AIMS).

#### References

- [1] J.E. Schiel, R. Mallik, S. Soman, K.S. Joseph, D.S. Hage, *J. Sep. Sci.* 29 (2006) 719.
- [2] T.M. Phillips, *LC Mag.* 3 (1985) 962.
- [3] T.M. Phillips, *Adv. Chromatogr.* 29 (1989) 133.
- [4] M. De Frutos, F.E. Regnier, *Anal. Chem.* 65 (1993) 17A.
- [5] D.S. Hage, *J. Chromatogr. B* 715 (1998) 3.
- [6] D.S. Hage, *Clin. Chem.* 45 (1999) 593.
- [7] G.T. Hermanson, A.K. Mallia, P.K. Smith, *Immobilized Affinity Ligand Techniques*, Academic Press, New York, 1992.
- [8] P.O. Larsson, *Methods Enzymol.* 104 (1984) 212.
- [9] J.W. Eveleigh, D.E. Levy, *J. Solid Phase Biochem.* 2 (1977) 45.
- [10] W. Clarke, J.D. Beckwith, A. Jackson, B. Reynolds, E.M. Karle, D.S. Hage, *J. Chrom. A* 888 (2000) 13.
- [11] C.T. Kresge, M.E. Leonowicz, W.J. Roth, J.C. Vartuli, J.S. Beck, *Nature* 359 (1992) 710.
- [12] A. Galarneau, J. Iapichella, K. Bonhomme, F. Di Renzo, P. Kooyman, O. Terasaki, F. Fajula, *Adv. Funct. Mater.* 16 (2006) 1657.
- [13] C. Petitto, A. Galarneau, M.-F. Driole, B. Chiche, B. Alonso, F. Di Renzo, F. Fajula, *Chem. Mater.* 15 (2005) 2120.
- [14] B. Lefevre, A. Galarneau, J. Iapichella, C. Petitto, F. Di Renzo, F. Fajula, Z. Bayram-Hahn, R. Skudas, K. Unger, *Chem. Mater.* 17 (2005) 601.
- [15] T. Martin, A. Galarneau, F. Di Renzo, F. Fajula, D. Plee, *Angewandte Chemie, Int. Ed.* 41 (2002) 2590.
- [16] J. Iapichella, J.-M. Meneses, I. Beurroies, R. Denoyel, Z. Bayram-Hahn, K. Unger, A. Galarneau, *Microporous Mesoporous Mater.* 102 (2007) 111.
- [17] A. Galarneau, J. Iapichella, D. Brunel, F. Fajula, Z. Bayram-Hahn, K.K. Unger, G. Puy, C. Demesmay, J.L. Rocca, *J. Sep. Sci.* 29 (2006) 844.
- [18] T. Martin, A. Galarneau, F. Di Renzo, D. Brunel, F. Fajula, S. Heinisch, G. Creter, J.-L. Rocca, *Chem. Mater.* 16 (2004) 1725.
- [19] D.Y. Zhao, J.L. Feng, Q.S. Huo, N. Melosh, G.H. Fredrickson, B.F. Chmelka, B.G.D. Stucky, *G. D. Science* 279 (1998) 548.
- [20] D.Y. Zhao, Q.S. Huo, J.L. Feng, B.F. Chmelka, G.D. Stucky, *J. Amer. Chem. Soc.* 120 (1998) 6024.
- [21] A. Galarneau, H. Cambon, F. Di Renzo, R. Ryoo, M. Choi, F. Fajula, *New J. Chem.* 27 (2003) 73.
- [22] A. Galarneau, H. Cambon, F. Di Renzo, F. Fajula, *Langmuir* 17 (2001) 8328.
- [23] A. Katiyar, L. Ji, P. Smirniotis, N.G. Pinto, *J. Chrom. A* 1069 (2005) 119.
- [24] F. Kleitz, S.H. Choi, R. Ryoo, *Chem. Comm.* 17 (2003) 2136.
- [25] T.-W. Kim, F. Kleitz, B. Paul, R. Ryoo, *J. Amer. Chem. Soc.* 127 (2005) 7601.
- [26] Y. Ma, L. Qi, J. Ma, Y. Wu, O. Liu, H. Cheng, *Coll. Surf. A: Physicochem. Eng. Aspects* 229 (2003) 1.
- [27] P. Schmidt-Winkel, W.W. Lukens Jr., D. Zhao, P. Yang, B.F. Chmelka, G.D. Stucky, *J. Am. Chem. Soc.* 121 (1999) 254.
- [28] P. Schmidt-Winkel, W.W. Lukens Jr., P. Yang, D.I. Margolese, J.S. Lettow, J.Y. Ying, G.D. Stucky, *Chem. Mater.* 12 (2000) 686.
- [29] Y. Han, S.S. Lee, J.J. Ying, *Chem. Mater.* 19 (2007) 2292.
- [30] G. Renard, M. Mureseanu, A. Galarneau, D.A. Lerner, D. Brunel, *New J. Chem.* 29 (2005) 912.
- [31] (a) J.C.P. Broekhoff, J.H. de Boer, *J. Catal.* 9 (1967) 8 ;  
(b) J.C.P. Broekhoff, J.H. de Boer, *J. Catal.* 10 (1968) 377.
- [32] A. Galarneau, D. Desplandier, R. Dutartre, F. Di Renzo, *Microporous Mesoporous Mater.* 27 (1999) 297.
- [33] J. Rouquerol, L. Davy, *Thermochim. Acta* 24 (1978) 391.
- [34] S.J. Gregg, K.S.W. Sing, *Adsorption, Surface Area and Porosity*, Academic Press, London, 1982.